Effect of a Compressive Uniaxial Strain on the Critical Current Density of Grain Boundaries in Superconducting $YBa_2Cu_3O_{7-\delta}$ Films

D. C. van der Laan*
Department of Physics, University of Colorado, Boulder, Colorado 80309, USA
National Institute of Standards and Technology, Boulder, Colorado 80305, USA

T. J. Haugan and P. N. Barnes
Air Force Research Laboratory, Wright-Patterson AFB, Ohio 45433-7919, USA
(Received 27 January 2009; published 9 July 2009)

The mechanism by which grain boundaries impede current flow in high-temperature superconductors has resisted explanation for over two decades. We provide evidence that the strain fields around grain boundary dislocations in $YBa_2Cu_3O_{7-\delta}$ thin films substantially suppress the local critical current density J_c. The removal of strain from the superconducting grain boundary channels by the application of compressive strain causes a remarkable increase in J_c. Contrary to previous understanding, the strain-free J_c of the grain boundary channels is comparable to the intrinsic J_c of the grains themselves.

DOI: 10.1103/PhysRevLett.103.027005 PACS numbers: 74.25.Fy, 74.25.Ld, 74.72.Bk, 74.78.Bz

Grain boundaries in high-temperature superconductors are of special interest with respect to the influence of structural composition and lattice strain on superconductivity. The mismatch between the crystalline structure of grains at the grain boundary results in periodic dislocations, where strain fields reduce the order parameter and locally drive the material into the normal state [1–3]. The spacing between dislocations is reduced with increased grain boundary angle, and the grain boundary critical current density ($J_{c,GB}$) decreases exponentially with angle [4,5]. The strong superconducting coupling across the boundary is lost when the nonsuperconducting cores at dislocations overlap [6]. At that point, the dominant mechanisms that limit $J_{c,GB}$ include band bending [7], a reduced charge carrier concentration [5,8], and a reduced coupling of the $d_{x^2-y^2}$-wave functions at both sides of the boundary [9].

So far, attempts to influence the grain boundary coupling have concentrated on changing the chemical composition by doping the grains [10] or the grain boundaries [11]. One of the most striking results is obtained by use of calcium doping in $YBa_2Cu_3O_{7-\delta}$ (YBCO), where substitution of Y^{3+} by Ca^{2+} at grain boundaries results in a reduction of the interface potential and a significant increase in $J_{c,GB}$ [12–14]. Doping affects both the charge carrier concentration and the strain fields at grain boundaries, which makes it hard to determine to what extent the increase in $J_{c,GB}$ is due to a reduction in grain boundary strain.

Strain plays a major role in current blocking at grain boundaries in high-temperature superconductors. Strain fields around dislocations that exceed approximately 1% prevent the transformation from a nonsuperconducting tetragonal structure to a superconducting orthorhombic structure during film growth, thereby strongly reducing the superconducting cross section of the grain boundary [2]. Residual strain from the dislocations is expected to have a large impact on the remaining superconducting cross section of the grain boundary, even after film growth, but its exact role remains unknown.

To obtain an accurate understanding of grain boundary transport, it is vital to understand the exact role of dislocation strain fields in grain boundary superconductivity. In this Letter, the effect of strain on $J_{c,GB}$ is determined by applying compressive strain to the grain boundary while other grain boundary mechanisms remain unaffected.

YBCO thin films were deposited by pulsed-laser deposition onto single-crystal and bicrystalline $SrTiO_3$ (STO) substrates. The bicrystalline substrates had symmetric [001]-tilt grain boundaries of 4°, 6°, 7.5°, and 12° that were oriented across the width of the 4 mm by 12 mm substrate. A 200 μm wide and 800 μm long microbridge was patterned along the length of the substrates in each sample by standard photolithographic methods following the deposition of an approximately 200 nm to 350 nm thick YBCO layer. All samples were close to being optimally doped, with critical temperatures of the grains ranging from 90.5 to 90.9 K. Experimental parameters for YBCO film deposition were described in detail in previous studies [15,16].

The substrates were glued into a 4 mm by 12 mm slot that was machined in a Cu-Be bending beam. Compressive strain was applied along the length of the films in liquid nitrogen by bending the beam in a 4-point bender [17]. The applied strain was measured directly with a strain gage mounted on top of the bending beam. The strain transfer from the bending beam to the substrate was confirmed with one sample by mounting a small strain gage on top of the substrate, next to the superconducting bridge. The critical current of the films at each strain level was determined within 0.5% uncertainty by use of a transport current and

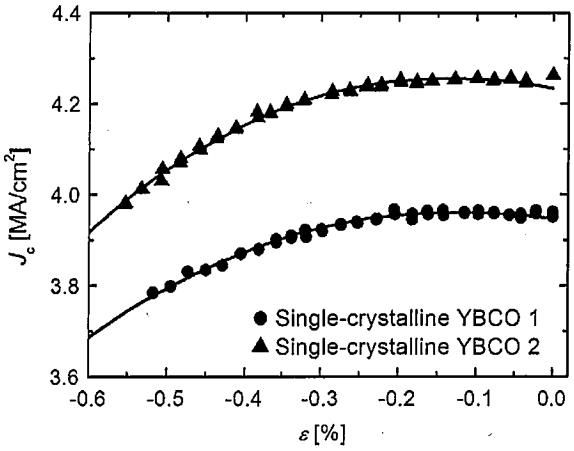

FIG. 1. The reversible change in J_c with uniaxial compressive strain that is measured in two YBCO thin films that were deposited on single-crystalline STO substrates. The solid lines are the strain dependence of the intragrain J_c, as described by Eq. (1).

an electric field criterion of 1 μV/cm for the case of single-crystal films, or a voltage criterion of 1 μV for the case of bicrystalline films.

The critical current density of two different YBCO thin films that were deposited on single-crystal STO substrates decreases when uniaxial compressive strain is applied (Fig. 1). The films have an initial J_c of 3.96 and 4.26 MA/cm^2, which is reduced to 3.79 and 4.05 MA/cm^2 at -0.5% strain. This change is not due to cracking in the film, and is fully reversible. The reversibility of the change in J_c is confirmed on a number of samples by partly releasing the compressive strain. The samples shown in Fig. 1 were not unloaded, because of the high chance of breaking the sample during strain cycling. The reversibility of the samples in Fig. 1 was confirmed by comparing the data with those samples that were unloaded. The transition from reversible to irreversible degradation in J_c with strain is very abrupt, where J_c is reduced by at least 25% between two adjacent strain points.

As is shown by the solid lines in Fig. 1, the strain dependence of J_c can be described accurately by use of a power-law fitting function of the form

$$J_c(\varepsilon) = J_c(\varepsilon_{m,G})(1 - a|\varepsilon - \varepsilon_{m,G}|)^b. \quad (1)$$

Here, $J_c(\varepsilon_{m,G})$ is the maximum critical current density that is reached when the YBCO layer experiences zero strain, which occurs at an applied strain of ε_m. The constants a, which is related to the strain sensitivity of the sample, and b, which defines the overall form of the power-law fitting function, remain fixed at $a = 7613$ and $b = 2.16$. These values follow from a global fit of the experimental data according to Eqs. (1) and (3) (below). The parameters of Eq. (1) are listed in Table I and confirm that the strain dependence of both YBCO films is identical [only the values of $J_c(\varepsilon_{m,G})$ differ between films]. Note that the location of the J_c peak according to the fit of Eq. (1) does not occur at zero applied strain, but at an applied strain of about -0.12%. This is due in part to the mismatch in thermal expansion coefficients of the YBCO film and the STO substrate, and is due in part to the small difference in lattice constants of both materials [18,19]. The strain dependence of J_c of the thin films is similar to that in YBCO coated conductors [20,21].

TABLE I. Parameter values for Eqs. (1) and (3).

	$J_c(\varepsilon_{m,G})$ (MA/cm^2)	$J_c(\varepsilon_{m,GB})$ (MA/cm^2)	$\varepsilon_{m,G}$ (%)	$\varepsilon_{m,GB}$ (%)
Single-crystalline YBCO-1	3.96	...	−0.13	...
Single-crystalline YBCO-2	4.26	...	−0.11	...
4° GB	...	6.73	...	−0.90
6° GB-1	...	7.61	...	−0.96
6° GB-2	...	9.60	...	−0.87
7.5° GB-1	...	5.48	...	−0.65
7.5 GB-2	...	3.94	...	−0.85
12° GB	...	3.82	...	−0.43

The effect of uniaxial compressive strain on the critical current density of four bicrystalline YBCO thin films is presented in Fig. 2. The strain is applied along the length of the films, perpendicular to the grain boundaries. The rate at which $J_{c,GB}$ increases depends on the angle of the grain boundary, and surprisingly is highest for the smallest grain boundary angle studied in our experiment. For the 12° grain boundary, $J_{c,GB}$ reaches a maximum at approximately -0.35% strain, as is clearly seen in Fig. 3.

To understand the strain dependence of $J_{c,GB}$, the superconducting channels between grain boundary dislocations were studied more closely. The nonsuperconducting dislocation cores reduce the superconducting cross section of

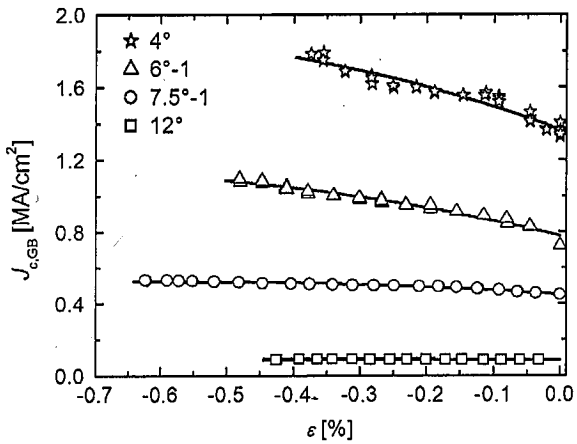

FIG. 2. The reversible change in $J_{c,GB}$ with uniaxial compressive strain that is measured in four thin film YBCO grain boundaries, with angles of 4°, 6° (film 6° GB-1 in Table I), 7.5° (film 7.5° GB-1 in Table I), and 12°. The solid lines are the critical current density according to Eq. (3).

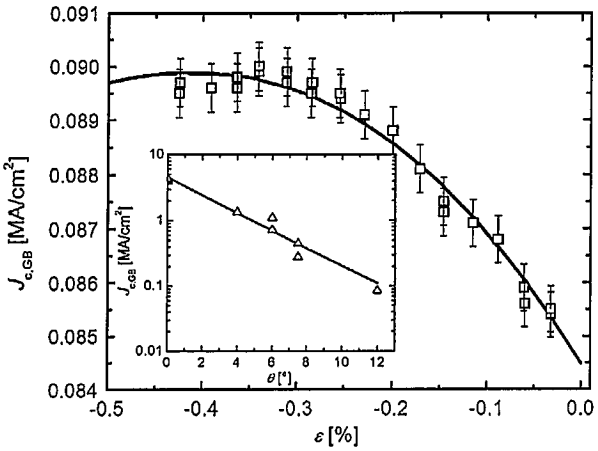

FIG. 3. The reversible change in $J_{c,GB}$ with uniaxial compressive strain that is measured in a thin film YBCO grain boundary of 12°. The solid line represents the critical current density according to Eq. (3). The error bars represent a 0.5% uncertainty in J_c. The inset shows an exponential decrease in $J_{c,GB}$ as a function of grain boundary angle. The solid line represents Eq. (2), with $J_c(0) = 4.55$ MA/cm^2 and $\theta_0 = 3.2°$.

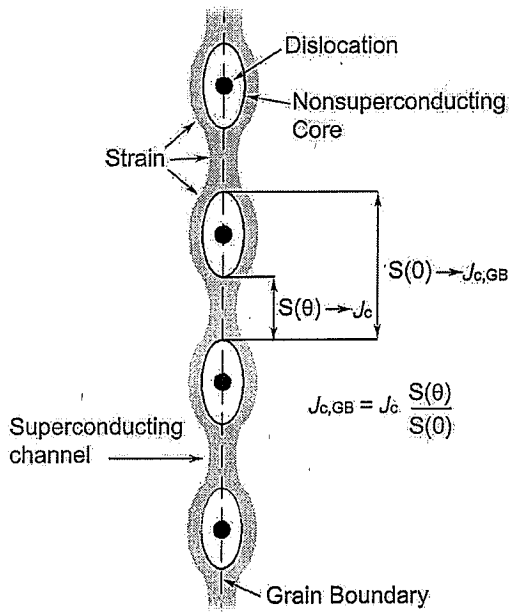

FIG. 4. Dislocations with nonsuperconducting cores reduce the superconducting cross section at grain boundaries, while strain fields that originate from the dislocations extend into the superconducting channels.

the boundary, as indicated in Fig. 4, where a schematic of a grain boundary is presented. The change in $J_{c,GB}$ with angle (θ) due to the dislocations is exponential [4,5]:

$$J_{c,GB}(\theta) = J_c(0)\frac{S(\theta)}{S(0)} = J_c(0)e^{(-\theta/\theta_0)}, \quad (2)$$

where $S(0)$ is the superconducting cross section of the grain boundary in the absence of any dislocations, and $S(\theta)$ is the reduced superconducting cross section in the presence of dislocations (see Fig. 4 and a detailed discussion in Ref. [3]). Equation (2) is experimentally demonstrated in the inset of Fig. 3.

The microstructure of the superconducting channels between dislocations is relatively undisturbed (although highly strained) and is expected to be identical to that of the grains. Remnant strain extends from the strain fields at the dislocations into these channels. Because the transformation to a superconducting orthorhombic structure no longer occurs during film growth when local strain exceeds approximately 1%, as described in Ref. [2], the residual strain in the grain boundary channels is estimated to be below approximately 1%. Based on this scenario, at low grain boundary angles, where the nonsuperconducting cores do not overlap, the strain dependence of J_c within the channels, and thus the strain dependence of $J_{c,GB}$, is expected to be identical to that of the intragrain J_c. The strain dependence of $J_{c,GB}$ is thus given by

$$J_{c,GB}(\varepsilon, \theta) = J_c(\varepsilon)\frac{S(\theta)}{S(0)} = J_c(\varepsilon_{m,GB})(1 - a|\varepsilon - \varepsilon_{m,GB}|)^b e^{(-\theta/\theta_0)}. \quad (3)$$

Here, $J_c(\varepsilon_{m,GB})$ is the maximum grain boundary critical current density that is reached when the channels experience no strain, which is expected to be comparable to $J_c(\varepsilon_{m,G})$ in the single-crystal YBCO films. The maximum occurs when the applied strain cancels the strain that exists within the channels (defined as $-\varepsilon_{m,GB}$). The constants a and b are obtained from a global fit of the data on both single-crystal and bicrystalline films, and are equal to $a = 7613$ and $b = 2.16$. The other fitting parameters that are used to fit the data are listed in Table I.

The strain dependence of $J_{c,GB}$ according to Eq. (3) is presented by the solid lines in Figs. 2 and 3. The model describes the data well with the parameter values listed in Table I, indicating that the strain dependence of the grain boundary and intragrain J_c's is comparable. The parameters of both Eq. (1) (intragrain films) and Eq. 3 (grain boundaries) were determined by forcing parameters a and b to be equal for all samples. Remarkably, the maximum J_c of the grain boundary channels is between 3.82 and 9.60 MA/cm^2, and is comparable to the maximum intragrain J_c (which ranges from 3.96 to 4.26 MA/cm^2). The spread in $J_c(\varepsilon_{m,GB})$ in Table I is likely due to the fact that the grain boundary angles in the YBCO layers are not clearly defined, due to grain boundary faceting [9], and this causes a spread in $J_c(\varepsilon_{m,GB})$ between samples (Table I).

The universal strain dependence of J_c on grains and symmetric [001]-tilt grain boundaries is outlined in Fig. 5. Here, the normalized J_c is presented as a function of intrinsic strain ε_0, defined as the strain that the YBCO layer experiences (a summation of the existing strain due to

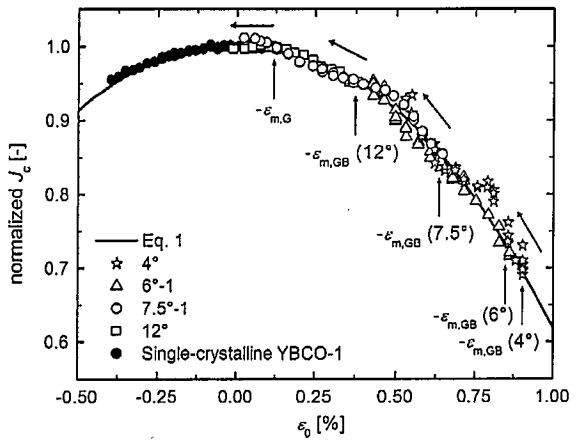

FIG. 5. Universal strain dependence of J_c as a function of intrinsic strain ε_0. The solid line represents Eq. (1), with $\varepsilon_{m,G} = 0$. The arrows that follow the curve indicate how existing lattice strain in the YBCO film is reduced when compressive strain is applied, and how J_c changes accordingly.

film growth and the applied strain). The normalized J_c is calculated by dividing the measured J_c of each grain boundary by $J_{c,GB}$ of Eq. (2) that are listed in Table I. Included in the figure are the $J_c(\varepsilon)$ data of a single-crystalline YBCO film and grain boundaries of angles 4°, 6°, 7.5°, and 12°. The YBCO films that were deposited on single-crystalline YBCO are under about 0.12% tensile strain, due to a mismatch in lattice constants and thermal expansion coefficient between YBCO and STO. The YBCO layer at grain boundaries experiences an additional strain caused by the strain fields that extend from the grain boundary dislocations into the superconducting channels, which will reduce T_c and J_c even further from their maximum values. The tensile strain that is present at the grain boundary channels ($-\varepsilon_{m,GB}$) is highest at low angles (ranging from 0.87% to 0.96% for 4° and 6°) and is reduced to 0.43% when the grain boundary angle is increased to 12°. The overall strain in the YBCO film is reduced by applying compressive strain. It is expected that J_c of the low-angle grain boundaries will reach its maximum when the applied compressive strain is increased further, as it does with the 12° grain boundary. According to Eq. (3), the 4° grain boundary is expected to have a maximum $J_{c,GB}$ of 1.93 MA/cm^2 at zero intrinsic strain, and likewise the 6° grain boundaries between 1.17 and 1.48 MA/cm^2 and the 7.5° grain boundaries between 0.38 and 0.53 MA/cm^2. Whether the observed strain dependence of the critical current holds for all low-angle grain boundaries in general is unknown, since only symmetric [001]-tilt grain boundaries have been studied.

In conclusion, J_c and the strain dependence of J_c of the superconducting channels at low symmetric [001]-tilt grain boundary angles are surprisingly identical to those of the grains. The results and analysis show that superconducting grain boundary channels are under tensile strain caused by the grain boundary and dislocation cores, which lower J_c, in addition to the exponential drop in J_c caused by the nonsuperconducting dislocation cores. The intrinsic strain of YBCO grain boundaries can be reduced significantly by applying *in situ* compressive strain, which results in a large increase in J_c.

The authors would like to thank Hans Hilgenkamp, Jochen Mannhart, and Jack Ekin for their technical input and fruitful discussions. This work was supported in part by the U.S. Department of Energy, Office of Electricity Delivery and Energy Reliability.

*danko@boulder.nist.gov

[1] D. Dimos, P. Chaudhari, and J. Mannhart, Phys. Rev. B **41**, 4038 (1990).
[2] M. F. Chisholm and S. J. Pennycook, Nature (London) **351**, 47 (1991).
[3] A. Gurevich and E. A. Pashitskii, Phys. Rev. B **57**, 13 878 (1998).
[4] D. Dimos *et al.*, Phys. Rev. Lett. **61**, 219 (1988).
[5] H. Hilgenkamp and J. Mannhart, Appl. Phys. Lett. **73**, 265 (1998).
[6] M. F. Chisholm and D. A. Smith, Philos. Mag. A **59**, 181 (1989).
[7] H. Hilgenkamp and J. Mannhart, Rev. Mod. Phys. **74**, 485 (2002).
[8] J. Mannhart and H. Hilgenkamp, Supercond. Sci. Technol. **10**, 880 (1997).
[9] H. Hilgenkamp and J. Mannhart, Phys. Rev. B **53**, 14 586 (1996).
[10] Z. Wen and H. Abe, Supercond. Sci. Technol. **9**, A76 (1996).
[11] Z. G. Ivanov *et al.*, Physica (Amsterdam) **194B**, 2187 (1994).
[12] J. Mannhart *et al.*, Physica (Amsterdam) **341C**, 1393 (2000).
[13] R. F. Klie *et al.*, Nature (London) **435**, 475 (2005).
[14] G. Hammerl *et al.*, Nature (London) **407**, 162 (2000).
[15] T. Haugan *et al.*, Nature (London) **430**, 867 (2004).
[16] T. Haugan *et al.*, Physica (Amsterdam) **397C**, 47 (2003).
[17] D. C. van der Laan *et al.* (to be published).
[18] J.-P. Locquet *et al.*, Nature (London) **394**, 453 (1998).
[19] H. Y. Zhai and W. K. Chu, Appl. Phys. Lett. **76**, 3469 (2000).
[20] D. C. van der Laan and J. W. Ekin, Appl. Phys. Lett. **90**, 052 506 (2007).
[21] M. Sugano *et al.*, Physica (Amsterdam) **463C**, 742 (2007).